Inorg. Chem. **2003**, *42*, 1701–1706

Bonding Coordination Requirements Induce Antiferromagnetic Coupling between *m*-Phenylene Bridged *o*-Iminosemiquinonato Diradicals

Andrea Dei,*,† Dante Gatteschi,† Claudio Sangregorio,† Lorenzo Sorace,†,‡ and Maria G. F. Vaz†

Department of Chemistry, University of Florence, UdR INSTM, Sesto Fiorentino, Italy, and CNRS-LCMI 25, Avenue des Martyrs, 38042 Grenoble, France

Received November 7, 2002

Triply bridged bis-iminodioxolene dinuclear metal complexes of general formula M_2(diox–diox)$_3$, with M = Co, Fe, have been synthesized using the bis-bidentate ligand *N*,*N*′-bis(3,5-di-*tert*-butyl-2-hydroxyphenyl)-1,3-phenylenediamine. These complexes were characterized by means of X-ray, HF-EPR, and magnetic measurements. X-ray structures clearly show that both complexes can be described as containing three bis-iminosemiquinonato ligands acting in a bis-bidentate manner toward tripositive metal ions. The magnetic data show that both of these complexes have singlet ground states. The observed experimental behavior indicates the existence of intraligand antiferromagnetic interactions between the three pairs of *m*-phenylene units linked iminosemiquinonato radicals ($J = 21$ cm^{-1} for the cobalt complex and $J = 11$ cm^{-1} for the iron one). It is here suggested that the conditions for the ferromagnetic coupling that is expected to characterize the free diradical ligand are no longer satisfied because of the severe torsional distortion induced by the metal coordination.

Introduction

Paramagnetic radical ligands are of considerable interest for the design of molecule-based magnetic materials,[1−6] in particular those that can bridge pairs of metal ions, thus opening the way to extended magnetic structures.[7−10] A class of ligands that have been used for this purpose are the trimethylene-type and *m*-phenylene-type bis-semiquinonates, in which the two paramagnetic moieties are ferromagnetically coupled to give a triplet ground state.[11−15] The ferromagnetic coupling originates from the nondisjoint nature of the nonbonding molecular orbitals of the biradicals.[16] Following this paradigm, some of us have recently shown how this approach can be extended to trinuclear metal complexes using a properly designed tris-dioxolene ligand.[17]

Within this framework, we have synthesized the ligand *N*,*N*′-bis(3,5-di-*tert*-butyl-2-hydroxyphenyl)-1,3-phenylenediamine which, once partially or fully deprotonated, can act

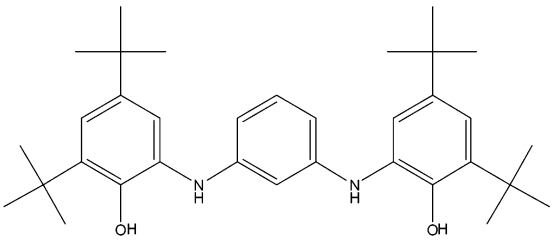

(**1**)

as a bis-bidentate ligand toward two different metal ions.

* Author to whom correspondence should be addressed. E-mail: andrea.dei@unifi.it.
† University of Florence.
‡ CNRS-LCMI.

(1) Gatteschi, D. *Adv. Mater.* **1994**, *6*, 635.
(2) Kahn, O. *Adv. Inorg. Chem.* **1995**, *43*, 179.
(3) Kahn, O. *Molecular Magnetism*; VCH: New York, 1993.
(4) Caneschi, A.; Gatteschi, D.; Rey, P. *Prog. Inorg. Chem.* **1991**, *39*, 331.
(5) Iwamura, H. *Pure Appl. Chem.* **1987**, *59*, 1595
(6) Lahti, P. M. *Magnetic Properties of Organic Materials*; Marcel Dekker: New York, 1999.
(7) Iwamura, H.; Inoue, K.; Hayamizu, T. *Pure Appl. Chem.* **1996**, *68*, 243.
(8) Inoue, K.; Hayamizu, T.; Iwamura, H.; Hashizume, D.; Ohashi, Y. *J. Am. Chem. Soc.* **1996**, *118*, 1803.
(9) Fegy, K.; Luneau, D.; Ohm, T.; Paulsen, C.; Rey, P. *Angew. Chem., Int. Ed. Engl.* **1998**, *37*, 1270.
(10) Misiolek, A. W.; Jackson, J. E. *J. Am. Chem. Soc.* **2001**, *123*, 4774.
(11) Shultz, D. A.; Boal, A. K.; Farmer, G. T. *J. Am. Chem. Soc.* **1997**, *119*, 3846.
(12) Shultz, D. A.; Boal, A. K.; Farmer, G. T. *J. Org. Chem.* **1998**, *63*, 9462
(13) Shultz, D. A.; Boal, A. K.; Campbell, N. P. *Inorg. Chem.* **1998**, *37*, 1540.
(14) Shultz, D. A.; Boal, A. K.; Driscoll, D. J.; Kitchin, J. R.; Tew, G. N. *J. Org. Chem.* **1995**, *60*, 3578.
(15) Caneschi, A.; Dei, A.; Lee, H.; Shultz, D. A.; Sorace, L. *Inorg. Chem.* **2001**, *40*, 408.
(16) Borden, W. T. In *Magnetic Properties of Organic Materials*; Lahti, P. M., Ed.; Marcel Dekker: New York, 1999, p 61.

10.1021/ic026160o CCC: $25.00
Published on Web 02/04/2003

Given the similarity of this molecule with catechols and *o*-phenylenediamines, it was expected that, once deprotonated, it could originate a redox chain in which some members were radicals or diradicals.[18,19] Indeed, if we indicate with the labels Cat, SQ, and Q the dinegative deprotonated form of the *o*-aminophenolate, the mononegative *o*-iminobenzosemiquinonate, and the neutral *o*-iminobenzoquinone fragments, respectively, then the five-members redox chain involving a sequence of four one-electron oxidation processes will be of the type

$$\text{Cat}-\text{Cat} \overset{-e^-}{\rightleftharpoons} \text{SQ}-\text{Cat} \overset{-e^-}{\rightleftharpoons} \text{SQ}-\text{SQ} \overset{-e^-}{\rightleftharpoons} \text{Q}-\text{SQ} \overset{-e^-}{\rightleftharpoons} \text{Q}-\text{Q}$$

in analogy with what has been already observed in a similar *m*-phenylene-bis(dioxolene) molecule.[11−15] The third member of the above redox chain, i.e., the dinegative diradical SQ−SQ species, is expected to have a triplet ground state according to the considerations mentioned above.

We investigated the coordination behavior of this ligand toward 3d metal ions with the goal of synthesizing systems in which ferromagnetically coupled diradicals would act as bis-bidentate ligands toward two different metal acceptors. We hoped to obtain ferromagnetically coupled extended structures, but on the contrary, we obtained dinuclear metal species. Indeed, the crystal structures of the cobalt and iron complexes can be formulated as $M_2(SQ-SQ)_3$, the metal ions being six-coordinated. The magnetic properties of the two compounds suggest that the severe distortions induced by the metal coordination can actually break the conditions for the ferromagnetic coupling that is expected to characterize the SQ−SQ diradical ligand. This possibility was theoretically predicted[16] but never observed in metal complexes.

Experimental Section

Synthesis. The ligand *N*,*N*′-bis(3,5-di-*tert*-butyl-2-hydroxyphenyl)-1,3-phenylenediamine was synthesized using the same procedure followed for the synthesis of the anilino-4,6-di-*tert*-butylphenol analog.[20−22] A short account of the synthetic procedure has been already reported.[23] 1,3-Phenylenenediamine (10 mmol) was allowed to react with 3,5-di-*tert*-butyl-catechol (20 mmol) in *n*-heptane (50 mL) in the presence of triethylamine (1 mL). The resulting mixture was refluxed for 5 h and then cooled. A gray-brown solid precipitated and was filtered and then recrystallized from acetonitrile−acetone mixtures. Yield 70%. (Anal. Found C 78.71, H 8.94, N 5.30; $C_{34}H_{48}O_2N_2$ requires C 79.02, H 9.36, N 5.42.) The iron and cobalt complexes were prepared by mixing the chloride of the appropriate divalent metal ion and the above ligand in the stoichiometric ratio of 1:1.5 in acetonitrile and then refluxing the resulting mixture for 3 h in the presence of triethylamine. The resulting solid products were filtered and washed with acetonitrile. They were then dissolved in $CHCl_3$, the resulting suspensions were filtered, and equal volumes of acetonitrile were added to the filtrates. The undissolved compounds are not well characterized metal oxides. Deep-green and deep-brown crystals for the iron and cobalt complexes, respectively, were obtained after 24 h. Suitable crystals for diffractometric analysis were obtained by slow evaporation of the solutions of the pure products in the same solvent mixtures. Although, in both cases, these crystals gave quite satisfactory X-ray diffraction patterns, both magnetic and EPR investigations evidenced the presence of small amounts of magnetic impurities. ($Co_2C_{108}H_{141}N_9O_6$: calcd C 73.98, H 8.03, N 5.07, Co 7.12; found C 72.97, H 7.94, N 5.25, Co 7.10. $Fe_2C_{102}H_{132}N_9O_6$: calcd C 74.25, H 8.06, N 5.09, Fe 6.77; found C 73.21, H 7.78, N 4.88, Fe 6.30).

Physical Measurements. Magnetic measurements were performed on a polycrystalline powder using a Cryogenic S600 SQUID magnetometer. To minimize the presence of magnetic impurities, the samples were obtained by grinding the crystals used for the X-ray analysis. Measurements were corrected for the diamagnetic contribution calculated from Pascal's constants. Susceptibility data were fit by minimizing the sum of the squares of the deviation of the computed χT values from the experimental values using a Simplex minimization procedure. The theoretical susceptibilities were calculated employing CLUMAG.[24]

HF-EPR spectra of $Co_2(SQ-SQ)_3$ were recorded on a home-built spectrometer equipped with a Gunn diode working at a fundamental frequency of 95 GHz with double and triple harmonic generation at the Grenoble High Magnetic Field Laboratory.[25] The sample was pressed into a pellet to prevent preferential orientation of the crystallites. Simulations of HF-EPR spectra were obtained by full diagonalization of the spin Hamiltonian matrix, using a previously described calculation procedure.[26]

X-ray data were collected on a CCD-1K three-circle Bruker diffractometer using Cu Kα radiation and a Göbel-mirror monochromator. Intensities were corrected for absorption (SADABS). Structures were successfully solved by direct methods (SIR97),[27] which gave the positions of most of the non-hydrogen atoms. The remaining atoms were identified by successive Fourier difference syntheses using SHELXL97,[28] and the hydrogen atoms were added in calculated positions assuming idealized bond geometries, except for some H atoms of the *m*-phenylene ring for $Co_2(SQ-SQ)_3$ that were located on a difference map. Anisotropic thermal factors were used for 118 of the 125 non-hydrogen atoms for $Co_2(SQ-SQ)_3$ and for 115 of 116 for $Fe_2(SQ-SQ)_3$. Details of crystal data collection and structure refinement for both compounds are given in Table 1.

Results

Structural Characterization of $Co_2(SQ-SQ)_3$ and $Fe_2(SQ-SQ)_3$. Crystallographic characterization of $Co_2(SQ-SQ)_3$ and $Fe_2(SQ-SQ)_3$ shows the dinuclear nature of these compounds. The X-ray crystal structure of the cobalt complex is shown in Figure 1.

(17) Caneschi, A.; Dei, A.; C. Mussari, P.; Shultz, D. A.; Sorace, L.; Vostrikova, K. E. *Inorg. Chem.* **2002**, *41*, 1086.
(18) Pierpont, C. G.; Lange, C. W. *Prog. Inorg. Chem.* **1994**, *41*, 331.
(19) Pierpont, C. G.; Buchanan, R. M. *Coord. Chem. Rev.* **1981**, *38*, 45.
(20) Maslovskaya, L. A.; Petrikevich, D. K.; Timoshchuk, V. A.; Shadyro, O. I. *Russ. J. Gen. Chem.* **1996**, *66*, 1842.
(21) Verani, C. N.; Gallert, S.; Bill, E.; Weyermüller, T.; Wieghardt, K.; Chaudhuri, P. *Chem. Commun*. **1999**, 1747.
(22) Chaudhuri, P.; Verani, C. N.; Bill, E.; Bothe, E.; Weyermüller, T.; Wieghardt, K. *J. Am. Chem. Soc*. **2001**, *123*, 2213.
(23) Dei, A.; Gatteschi, D.; Sangregorio, C.; Sorace, L.; Vaz, M. G. F. *Chem. Phys. Lett*. **2003**, *368*, 162.
(24) Gatteschi, D.; Pardi, L. *Gazz. Chim. Ital*. **1993**, *123*, 231.
(25) Muller, F.; Hopkins, M. A.; Coron, N.; Grynberg, M.; Brunel, L.; Martinez, C. G. *Rev. Sci. Instrum*. **1989**, *60*, 3681.
(26) Jacobsen, C. J. H.; Pedersen, E.; Villadsen, J.; Weihe, H. *Inorg. Chem*. **1993**, *32*, 1216.
(27) Altomare, A.; Burla, M. C.; Camalli, M.; Cascarano, G. L.; Giacovazzo, C.; Guagliardi, A.; Moliterni, A. G. G.; Polidori, G.; Spagna, R. *J. Appl. Crystallogr.* **1999**, *32*, 115.
(28) Sheldrick, G. M. *SHELXL97—Programs for Crystal Structure Analysis*, release 97-2; Institüt für Anorganische Chemie, Universität Göttingen, Göttingen, Germany, 1998.

Table 1. Crystal Data and Structure Refinement for $Co_2(SQ-SQ)_3$ and $Fe_2(SQ-SQ)_3$

	$Co_2C_{108}H_{141}N_9O_6$	$Fe_2C_{102}H_{132}N_9O_6$
formula weight	1779.16	1649.83
temperature	150(2) K	150(2) K
wavelength	1.541 78 Å	1.541 78 Å
crystal system, space group	monoclinic, $P2_1/c$	monoclinic, $C2/c$
unit cell dimensions	$a = 21.053(2)$ Å	$a = 40.491(18)$ Å
	$b = 17.524(2)$ Å	$b = 15.375(7)$ Å
	$c = 28.583(3)$ Å	$c = 32.260(14)$ Å
	$\alpha = 9.000(3)°$	$\alpha = 90.000(10)°$
	$\beta = 90.200(5)°$	$\beta = 92.010(10)°$
	$\gamma = 90.000(3)°$	$\gamma = 90.000(10)°$
volume	10 545(2) Å^3	20 071(15) Å^3
Z	4	4
calculated density	1.121 mg/m^3	1.092 mg/m^3
absorption coefficient	2.882 mm^{-1}	2.715 mm^{-1}
$F(000)$	3816	7088
crystal size	0.8 × 0.2 × 0.2 mm	0.5 × 0.2 × 0.15 mm
θ range for data collection	2.10−57.74°	2.74−50.64°
limiting indices	$-20 \le h \le 22$	$-40 \le h \le 39$
	$-17 \le k \le 18$	$-15 \le k \le 15$
	$-29 \le l \le 30$	$-29 \le l \le 32$
reflections collected/unique	35 353/13 365	23 241/10 035
	[R(int) = 0.0491]	[R(int) = 0.0736]
completeness to θ	57.74, 91.8%	50.64, 94.5%
refinement method	full-matrix least-squares on F^2	full-matrix least-squares on F^2
data/restraints/parameters	13 365/0/1122	10 035/0/1040
GOF on F^2	1.051	1.071
final R indices [$I > 2\sigma(I)$]	R1 = 0.0586	R1 = 0.1049
	wR2 = 0.1506	wR2 = 0.2458
R indices (all data)	R1 = 0.0755	R1 = 0.1520

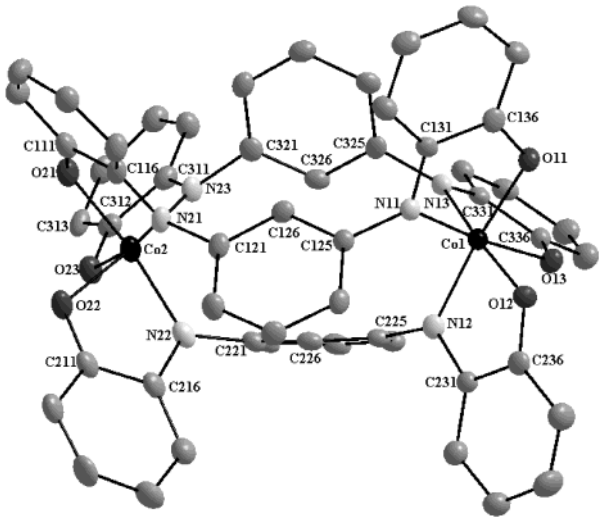

Figure 1. Molecular structure of $Co_2(SQ-SQ)_3$. Hydrogen atoms and *tert*-butyl groups are omitted for clarity. Thermal ellipsoids are shown at 50% probability.

Table 2. Bond Lengths (Å) for $Co_2(SQ-SQ)_3$ and $Fe_2(SQ-SQ)_3$

$Co_2C_{108}H_{141}N_9O_6$		$Fe_2C_{102}H_{132}N_9O_6$	
Co(1)−O(11)	1.895(3)	Fe(1)−O(11)	2.031(7)
Co(1)−O(12)	1.904(3)	Fe(1)−O(12)	2.014(6)
Co(1)−O(13)	1.878(2)	Fe(1)−O(13)	1.995(6)
Co(1)−N(11)	1.916(3)	Fe(1)−N(11)	2.072(7)
Co(1)−N(12)	1.933(3)	Fe(1)−N(12)	2.070(8)
Co(1)−N(13)	1.938(3)	Fe(1)−N(13)	2.140(8)
Co(2)−O(21)	1.893(3)	Fe(2)−O(21)	2.021(6)
Co(2)−O(22)	1.903(3)	Fe(2)−O(22)	2.027(6)
Co(2)−O(23)	1.901(3)	Fe(2)−O(23)	2.029(7)
Co(2)−N(21)	1.939(3)	Fe(2)−N(21)	2.085(8)
Co(2)−N(22)	1.918(3)	Fe(2)−N(23)	2.105(8)
Co(2)−N(23)	1.933(3)	Fe(2)−N(22)	2.129(7)
O(11)−C(136)	1.296(4)	O(11)−C(136)	1.298(11)
O(12)−C(236)	1.302(4)	O(12)−C(236)	1.289(11)
O(13)−C(336)	1.304(4)	O(13)−C(336)	1.305(10)
O(21)−C(111)	1.299(5)	O(21)−C(111)	1.281(10)
O(22)−C(211)	1.295(5)	O(22)−C(211)	1.311(11)
O(23)−C(312)	1.302(5)	O(23)−C(316)	1.304(11)
N(11)−C(131)	1.348(5)	N(11)−C(121)	1.424(11)
N(11)−C(125)	1.421(5)	N(11)−C(131)	1.347(12)
N(12)−C(231)	1.344(5)	N(12)−C(221)	1.410(11)
N(12)−C(225)	1.436(5)	N(12)−C(231)	1.352(11)
N(13)−C(331)	1.348(5)	N(13)−C(321)	1.440(11)
N(13)−C(325)	1.430(5)	N(13)−C(331)	1.335(11)
N(21)−C(116)	1.346(5)	N(21)−C(116)	1.372(12)
N(21)−C(121)	1.430(5)	N(21)−C(125)	1.426(12)
N(22)−C(216)	1.352(5)	N(22)−C(216)	1.369(12)
N(22)−C(221)	1.429(5)	N(22)−C(225)	1.409(12)
N(23)−C(311)	1.341(5)	N(23)−C(311)	1.328(11)
N(23)−C(321)	1.431(5)	N(23)−C(325)	1.396(12)
C(111)−C(116)	1.437(5)	C(111)−C(116)	1.435(13)
C(131)−C(136)	1.438(5)	C(131)−C(136)	1.463(14)
C(211)−C(216)	1.436(6)	C(211)−C(216)	1.444(13)
C(231)−C(236)	1.436(5)	C(231)−C(236)	1.421(13)
C(311)−C(316)	1.418(6)	C(311)−C(316)	1.446(13)
C(331)−C(336)	1.436(5)	C(331)−C(336)	1.478(13)

The view of the molecule shows the three ligands acting in a bis-bidentate manner toward two different pseudo-octahedral cobalt ions. As a result, both of the metal ions are facially coordinated to three deprotonated nitrogen atoms and three oxygen donor atoms. Selected bond distances for both compounds are reported in Table 2. The structural parameters are fully consistent with a bis[cobalt(III)-tris(*o*-iminosemiquinonato)] description of this derivative.[19,21,22] Indeed, the average values of the Co−N and Co−O bond distances are 1.93 and 1.89 Å, respectively, and agree well with the expectations for a tripositive low-spin metal acceptor. Further, the observed 1.30-Å average value for the C−O bond length is in the range usually observed for 3d metal−semiquinonato complexes.[18,19] Similar conclusions can be reached through an inspection of the C−C bond lengths, whose average value of 1.44 Å is again strongly indicative of radical character of the iminooxolene ring. The characters of the two C−N bonds linking the nitrogen donor atom to the iminooxolene and *m*-phenylene rings are significantly different from each other, the first one being 1.34 Å (C═N character) whereas the average value of the latter is 1.42 Å (C−N character). The observed results fully agree with those observed for a previously reported cobalt(III)-tris(iminosemiquinonato) complex.[21]

A relevant feature of this structure is the conformation of the iminosemiquinonato rings with respect to the linker *m*-phenylene rings. The dihedral angles between the planes containing the next-neighbor rings are significantly different from those expected for the free ligand (∼15−20°), as a result of the steric constraints imposed by the coordination to the metal centers (Table 3). This is expected to deeply affect the magnetic properties of the bis(iminosemiquinonato) diradical ligand. It is worth pointing out that each ligand presents two different values of this dihedral angle, one in the range 66.8−72.1° and the other in the range of 83.3−88.1°.

Notwithstanding numerous attempts at recrystallization we did not manage to obtain high quality crystals for $Fe_2(SQ-SQ)_3$. Thus, the resulting structure shown in Figure

Table 3. Selected Torsion Angles (degrees) for $Co_2(SQ-SQ)_3$ and $Fe_2(SQ-SQ)_3$

$Co_2C_{108}H_{141}N_9O_6$		$Fe_2C_{102}H_{132}N_9O_6$	
C(326)−C(321)−N(23)−C(311)	83.3(3)	C(326)−C(321)−N(13)−C(331)	73.3(4)
C(326)−C(325)−N(13)−C(331)	71.0(3)	C(326)−C(325)−N(23)−C(311)	70.3(3)
C(226)−C(221)−N(22)−C(216)	66.8(2)	C(226)−C(221)−N(12)−C(231)	87.9(2)
C(226)−C(225)−N(12)−C(231)	86.1(3)	C(226)−C(225)−N(22)−C(216)	52.3(3)
C(126)−C(121)−N(21)−C(116)	88.2(2)	C(126)−C(121)−N(11)−C(131)	74.1(2)
C(126)−C(125)−N(11)−C(131)	72.1(1)	C(126)−C(125)−N(21)−C(116)	79.5(3)

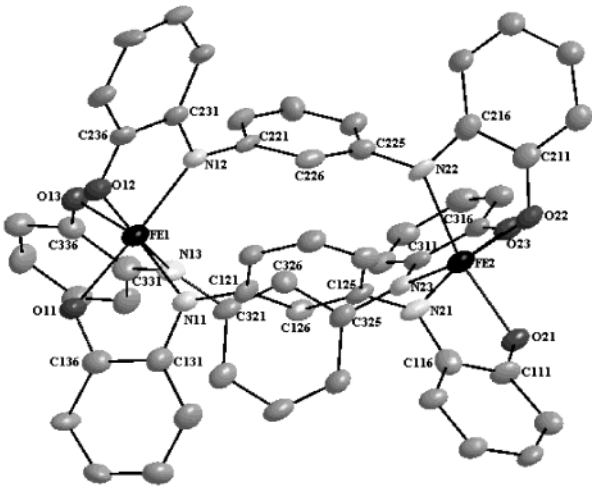

Figure 2. Molecular structure of $Fe_2(SQ-SQ)_3$. Hydrogen atoms and *tert*-butyl groups are omitted for clarity. Thermal ellipsoids are shown at 50% probability.

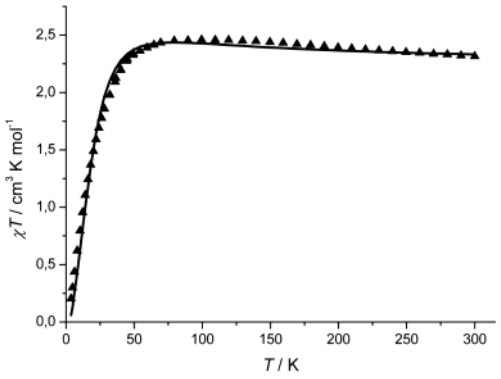

Figure 3. χT vs T curve for $Co_2(SQ-SQ)_3$ (full triangles) and best-fit curve (continuous line); see text for details.

2 is not of good quality (Table 1). At any rate, the main features are clear and provide a sufficient basis for the analysis of the magnetic behavior of this complex, to be discussed below. In particular, the bond lengths of the coordination spheres of the two metal ions are in good agreement with those expected for a tripositive iron ion in high-spin configuration, as further supported by Mössbauer spectroscopy (see the Supporting Information). In agreement with this oxidation state of the metal ions, the C−O, C−C, and C−N bond lengths of the ligands, reported in Table 2, are in the range expected for a bis-semiquinonato oxidation state of the ligand, as observed for the cobalt complex. The different nature of the C−N bond connecting the nitrogen atom to *m*-phenylene ring with respect to that connecting nitrogen to the iminosemiquinonato ring is again evidenced by the large differences in their bond lengths, averaging 1.42 Å (C−N character) and 1.35 Å (C═N character), respectively. On the other hand, a remarkable difference from the structure of the cobalt derivative lies in the dihedral angles formed by the next-neighbor rings (Table 3), which show a larger dispersion and a smaller average value.

Magnetic Properties of $Co_2(SQ-SQ)_3$ and $Fe_2(SQ-SQ)_3$. As pointed out in the Experimental Section, the products, even in crystalline form, were invariably affected by the presence of small amounts of coprecipitates. This problem was not removed even with samples obtained by grinding crystals suitable for diffractometric analysis. The impurities associated with both the Co and Fe derivatives turned out to be strongly magnetic, thus complicating the quantitative analysis of the magnetic behavior of the two complexes. The magnetic measurements of the isolated coprecipitates (Supporting Information) allowed us to estimate that their concentrations were lower than 2 and 1% for Co and Fe, respectively. The experimental χT vs T curves were then corrected to account for this contribution.

At room temperature, the χT value for $Co_2(SQ-SQ)_3$, shown in Figure 3, is 2.32 cm^3 K mol^{-1}, close to that expected for six uncorrelated $S = {}^1/_2$ spins (2.25 cm^3 K mol^{-1}), and its tendency is to slowly increase with decreasing temperature, thus approaching a maximum of 2.47 cm^3 K mol^{-1} around 120 K. Below this temperature, there is a decrease of χT, which reaches a value of 0.2 cm^3 K mol^{-1} at 4 K. These data clearly show that there are two types of coupling, ferromagnetic coupling, dominant at high temperature, and antiferromagnetic coupling, yielding a singlet ground state.

Even though the crystal structure shows that the iminosemiquinonato donors are not strictly equivalent, a satisfactory fit of the experimental data was obtained by assuming the simplest Hamiltonian

$$H = J_1(S_1S_2 + S_2S_3 + S_1S_3 + S_{1'}S_{2'} + S_{2'}S_{3'} + S_{1'}S_{3'}) + J_2(S_1S_{1'} + S_2S_{2'} + S_3S_{3'}) \quad (1)$$

where $S_i = {}^1/_2$ ($i = 1-3$, $1'-3'$) and S_i and $S_{i'}$ refer to the magnetic coupling between two iminosemiquinonato centers linked by the same *m*-phenylene moiety. Assuming $g_i = 2.00$ and TIP $= 200 \times 10^{-6}$ emu mol^{-1}, we found $J_1 = -27.6 \pm 2$ cm^{-1} and $J_2 = 21.1 \pm 0.4$ cm^{-1}. No acceptable fit was obtained if the signs of the J constants were inverted. With these values of the coupling constants, the first excited state was determined to be a triplet lying 9.9 cm^{-1} higher than the ground state.

In agreement with the quite small singlet−triplet gap, it is expected that, at higher fields, the low-lying triplet state would be either the ground state or very close to it. This is

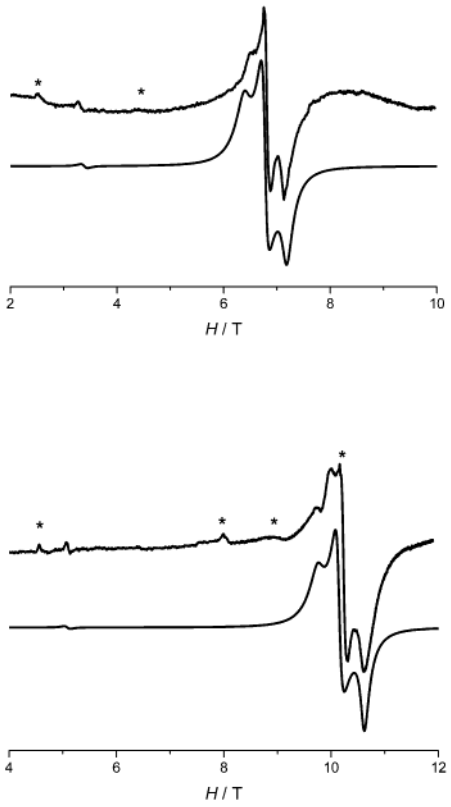

Figure 4. HF-EPR spectra of $Co_2(SQ-SQ)_3$ at 190 GHz (upper) and 285 GHz (lower) and 5 K. For each frequency, the upper curve is the experimental one, and the lower curve is the simulated one. The features marked with an asterisk were attributed to the magnetic coprecipitate. See text for details.

indeed confirmed by the observation of intense HF-EPR spectra at low temperatures and different frequencies (Figure 4). The spectra clearly show the features of a triplet species, with a $|\Delta M_S| = 2$ half-field transition and significant rhombic character evidenced by the main features around $g = 2$. The best simulations were obtained on the basis of the second-order spin Hamiltonian $H = \beta gSH + DS_z^2 + E(S_x^2 - S_y^2)$, with $D = +0.38 \pm 0.01$ cm^{-1}, $E/D = 0.29 \pm 0.01$, and $g_{iso} = 2.00$. These simulations reproduced fairly well the forbidden transition at half-field and the position and relative intensity of the rhombic signal around $g = 2.00$, whereas the features marked with an asterisk were attributed to the magnetic coprecipitate. The presence of the coprecipitate is also likely to be the cause of the small discrepancies observed in the line position for the transition around 6.5 T in the 190-GHz spectra.

At room temperature, the χT value of the iron derivative (Figure 5) clearly indicates that strong antiferromagnetic interactions are active. Indeed, the measured value of 2.1 cm^3 K mol^{-1} is much lower than that expected for the eight uncorrelated spins, and it is only slightly higher than that expected for two uncorrelated $S = 1$, spins which would result from the antiferromagnetic coupling of each iron spin to the three surrounding radicals. This interpretation, which is fully consistent with previous observation on iron(III)-semiquinonato complexes, is confirmed by the fact that χT decreases as the temperature is lowered to 180 K, where it reaches a plateau of 2.0 cm^3 K mol^{-1} corresponding to two

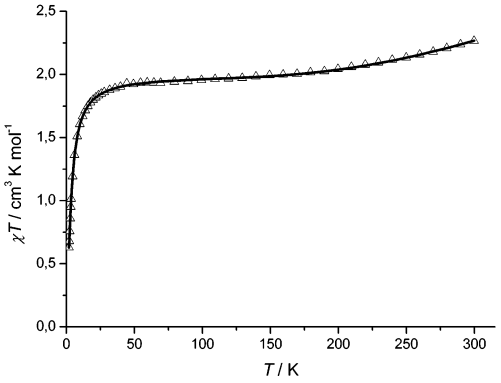

Figure 5. χT vs T curve for $Fe_2(SQ-SQ)_3$ (open triangles) and best-fit curve (continuous line). The best-fit parameters are reported in the text.

isolated $S = 1$ spins. Finally, the decrease observed below 40 K is readily attributed to the antiferromagnetic coupling that characterizes the two diradical moieties in analogy with what we have observed in the cobalt complex.

Even with the simplifying assumption of equivalent iminosemiquinonato ligands, a quantitative analysis of the magnetic properties in this case requires the use of a Hamiltonian involving at least three coupling constants

$$H = J_{FeSQ}(S_{Fe1}S_{SQ11} + S_{Fe1}S_{SQ21} + S_{Fe1}S_{SQ31} + S_{Fe2}S_{SQ12} + S_{Fe2}S_{SQ22} + S_{Fe2}S_{SQ32}) + J_{SQ-SQ}(S_{SQ11}S_{SQ12} + S_{SQ21}S_{SQ22} + S_{SQ31}S_{SQ32}) + J'_{SQ-SQ}(S_{SQ11}S_{SQ21} + S_{SQ21}S_{SQ31} + S_{SQ31}S_{SQ11} + S_{SQ12}S_{SQ22} + S_{SQ22}S_{SQ32} + S_{SQ32}S_{SQ12}) \quad (2)$$

where the indexes of SQ indicate the ith ligand and the position close to the jth Fe(III) ion; thus, J'_{SQ-SQ} identifies the coupling between radical moieties of different ligands occurring through Fe(III) ions, and J_{SQ-SQ} identifies the intraligand radical−radical interaction transmitted by the *m*-phenylene ring.

The best-fit curve was obtained by using $J_{Fe-SQ} = 340 \pm 8$ cm^{-1}, $J_{SQ-SQ} = 11 \pm 0.4$ cm^{-1}, and $J'_{SQ-SQ} = -168$ cm^{-1}. Even though this latter value is extremely large and out of the expected range for such systems, it should be stressed that, during the fitting procedure, it turned out that, given the strong antiferromagnetic coupling between Fe(III) and iminosemiquinonato, the value of J'_{SQ-SQ} did not affect the fit quality as long as it remained ferromagnetic (i.e., negative), and no appreciable correlation was observed between the value of J'_{SQ-SQ} and those of the two remaining constants. With these values of the coupling constants, the ground singlet state was found to be quite close in energy to the first two excited states, $S = 1$ and $S = 2$, lying 1.9 and 5.7 cm^{-1}, respectively, higher in energy.

Discussion

The tris-chelation of an asymmetric bidentate ligand affording a pseudoctahedral metal complex can occur in (i) meridional or (ii) facial fashion, i.e. The reported crystal structures of tris-*o*-semiquinonato and tris-*o*-iminosemiquinonato metal complexes show that the isomer with

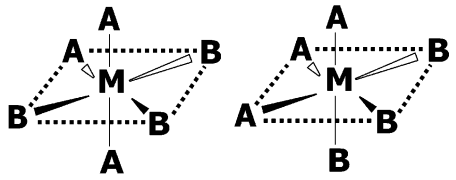

meridional coordination is generally favored,[21,29] and this experimental result can be easily understood by taking into account statistical considerations, electrostatic repulsion between the charged donor atoms, and nonbonding interactions between the coordinated ligands. In the present case, meridional coordination would afford a three-dimensionally connected structure. On the contrary, a facial isomer is formed, and so, a dinuclear structure is possible. Also, for this configuration, the conditions leading to ferromagnetic coupling, as observed for the previously reported tris-*o*-semiquinonato[29,30] and tris-*o*-iminosemiquinonato[21] metal complexes, are met. On the other hand, *m*-phenylene-based diradicals are expected to present ferromagnetic coupling between the two iminosemiquinonato moieties. The observed antiferromagnetic coupling between the diradical ligands in the $Co_2(SQ-SQ)_3$ and $Fe_2(SQ-SQ)_3$ complexes initially presents a significant discrepancy with respect to the expectations. This behavior can be explained by taking into account the large values of the dihedral angles between the planes containing the *m*-phenylene and iminosemiquinonato ligands. Indeed, although never observed for metal complexes, previous investigations on sterically hindered *m*-phenylene diradicals[31] showed that, as the torsion angles between the spin-bearing units and the bridging phenyl fragment planes increase, the energy gap between the diradical triplet ground states and the first excited singlet decreases and, in limiting cases, the relative energies of the two electronic states are inverted with respect to expectations. Thus, the observed singlet ground state of the diradical moiety results from the inhibition of electron delocalization of the spin-bearing units into the π system of the *m*-phenylene moiety, thus rendering inoperative any spin-polarization mechanism leading to the stabilization of the triplet state. This effect was clearly shown by Borden,[32] whose calculations indicate that the antiferromagnetic coupling between the two radicals is due to the mixing of the π^* SOMO of the diradicals with the appropriate σ orbitals of the phenylene moiety. In agreement with this picture, the observed antiferromagnetic coupling is larger for the cobalt derivative than for the iron one, because of the larger average dihedral angle characterizing the three-ring π system in the former complex.

Acknowledgment. The authors thank A.-L. Barra for technical assistance in recording HF-EPR spectra, J. D. Ardisson and W. A. A. Macedo for recording Mössbauer spectra, and S. Ciattini for assistance in X-ray data collection. EU-network 3MD and Molnanomag, CNR, and MIUR are gratefully acknowledged for financial support. M.G.F.V. gratefully acknowledges the Brazilian Conselho Nacional de Desenvolvimento Cientifico e Tecnologico (CNPq).

Supporting Information Available: CIF data files containing crystallographic information for complexes $Co_2(SQ-SQ)_3$ and $Fe_2(SQ-SQ)_3$, Mössbauer spectra for complex $Fe_2(SQ-SQ)_3$, and magnetic measurements of the coprecipitates. This material is available free of charge via the Internet at http://pubs.acs.org.

IC026160O

(29) Adams, D. M.; Rheingold, A. L.; Dei, A.; Hendrickson, D. N. *Angew. Chem., Int. Ed. Engl.* **1993**, *32*, 391.
(30) Ozarowski, A.; McGarvey, B. R.; El-Hadad, A.; Tian, Z.; Tuck, D. G.; Krovich, D. J.; DeFotis, G. C. *Inorg. Chem.* **1993**, *32*, 841.
(31) Shultz, D. A. In *Magnetic Properties of Organic Materials*; Lahti, P. M., Ed.; Marcel Dekker: New York, 1999, p 104.
(32) Ming-Shi Lee, S. F.; Hrovat, D. A.; Borden, W. T. *J. Am. Chem. Soc.* **1995**, *117*, 6727.